Ultraviolet photoluminescence in Gd-doped silica and phosphosilicate fibers

Y. Wang[1,a)], J. He[1], P. Barua[1], N. Chiodini[2], S. Steigenberger[3], M. I. M. Abdul Khudus[1,4], J.K.Sahu[1], M. Beresna[1], and G. Brambilla[1]

[1]*Optoelectronics Research Centre, University of Southampton, Southampton, SO17 1BJ, United Kingdom*

[2]*Dipartimento di Scienza dei Materiali, Università di Milano Bicocca, 20126, Milan, Italy*

[3]*National Oceanography Centre, University of Southampton Waterfront Campus, European Way, Southampton, SO14 3ZH, United Kingdom*

[4]*Photonics Research Centre, Department of Physics, Faculty of Science, University of Malaya, 50603 Kuala Lumpur, Malaysia*

Optical fiber lasers operating in the near infrared (IR) and visible spectral regions have relied on the spectroscopic properties of rare earth ions such as Yb^{3+}, Er^{3+}, Tm^{3+}, Nd^{3+} and Sm^{3+}. Here, we investigate Gd^{3+} doping in phosphosilicate and pure silica fibers using solution doping and sol-gel techniques respectively for potential applications in the ultraviolet (UV). Photoluminescence spectra for optical fiber bundles and fiber preforms were recorded and compared. Emissions at 312 nm (phosphosilicate) and 314 nm (pure silica) were observed when pumping to the Gd^{3+} ^6D_J, ^6I_J, and $^6P_{J=5/2,\ 3/2}$ energy levels. Oxygen deficient center was observed in solution doping sample with a wide absorption band centered at around 248 nm not affecting pumping to ^6I_J states.

Ultraviolet (UV) light sources have found numerous applications in medical science and engineering, such as disinfection, water purification, food manufacturing, UV curing and lithography[1-4], as short wavelengths have relatively high photon energy and provide high resolution. Currently, UV sources consist mostly of gas lasers[5], lamps or diodes[1], or rely on nonlinear optical processes, such as third/fourth harmonic generation or optical parametric oscillators (OPOs)[6-7]. Fiberized laser sources could be an attractive alternative to conventional UV sources. Fiber based light sources exhibit excellent beam quality, extraordinary brightness, small detrimental thermal effects and high temporal stability. Fiber lasers operating in the near infrared and visible mostly rely on the spectroscopic properties of rare earth ions[8]. High-power Yb^{3+}-doped

[a] Author to whom correspondence should be addressed. Electronic mail: yw11e13@soton.ac.uk.

fiber lasers at the wavelength of λ~1μm have found extensive applications in metal processing like welding, milling and marking[9-10]. Extension to the UV would benefit applications such as precise micromachining and processing/marking of insulators, which are usually energy inefficient when carried out with near IR lasers and would benefit from an improved optical absorption, higher resolution as well as minimized thermal damage.

Gd^{3+} has its first excited state located at a wavenumber $\tilde{\nu}$~32000 cm^{-1} above the ground level (Fig. 1a), corresponding to an UV emission at λ~312.5 nm. Simultaneously, silica glass, the host material, has various advantages including transparency in the UV down to λ~200nm[11-12], extraordinary mechanical strength, strong chemical and radiation resistance and compatibility with existing silica-based components. The silica network has a high phonon energy ($\tilde{\nu}$~1100 cm^{-1}), therefore transitions among the ^6D_J, ^6I_J and ^6P_J energy levels in Gd^{3+}-doped silica tend to be dominated by non-radiative multi-phonon relaxation due to the small energy gaps. Previous studies of Gd-doped samples in film, bulk and powder form under electron-beam, VUV and X-ray excitation[13-15] suggest that the emission at λ~312nm, given by the $^6P_{7/2} \rightarrow {}^8S_{7/2}$ transition, would be a promising candidate for the generation of light in the UV. The lifetime of the $^6P_{7/2}$ level has been found to be 5 ms in a sol-gel sample containing ~3 mol% of Gd[16]. Rapid thermal treatment on Gd-doped sol-gel silica bulk sample resulted in an enhancement in Gd^{3+} luminescence[17]. This work investigates the luminescence of Gd^{3+} in silica fibers as a possible candidate for the development of coherent solid state sources in the UV.

Two types of Gd^{3+}-doped fiber samples with a pure silica and a phosphosilicate core were studied. The phosphosilicate sample was fabricated using the modified chemical vapor deposition (MCVD) and solution doping techniques[18]. The core layer, formed by un-sintered porous soot, was deposited inside a silica tube (F-300, Heraeus) at the temperature T~1530 ºC by oxidizing the vapor-phase precursors $SiCl_4$ and $POCl_3$. The tube was subsequently soaked for about one hour in solution containing $GdCl_3 \cdot 6H_2O$ dissolved in methanol. The core layer was then sintered and the tube was collapsed into a preform with a silica cladding and a Gd^{3+}-doped phosphosilicate core. The dopant concentration along the preform core cross section was measured by energy-dispersive X-ray spectroscopy (EDX) in a sample cut from the fiber preform (Fig. 1b). The Gd^{3+} concentration reaches its maximum, >2000 ppm by mol, at a position 200 μm away from the preform center. The decreased concentration level at the preform center was attributed to the evaporation of P_2O_5 during the consolidation process, which also removed Gd^{3+}. The average atomic percentage of Gd^{3+} across the preform core cross section was determined as ~1170 ppm by mol. The preform was subsequently pulled into an optical fiber at the temperature T~2040 ºC. The fiber had core and cladding diameters of d_{co}=5.8 μm and d_{cl}=125 μm, respectively, and a numerical aperture (NA) of 0.13.

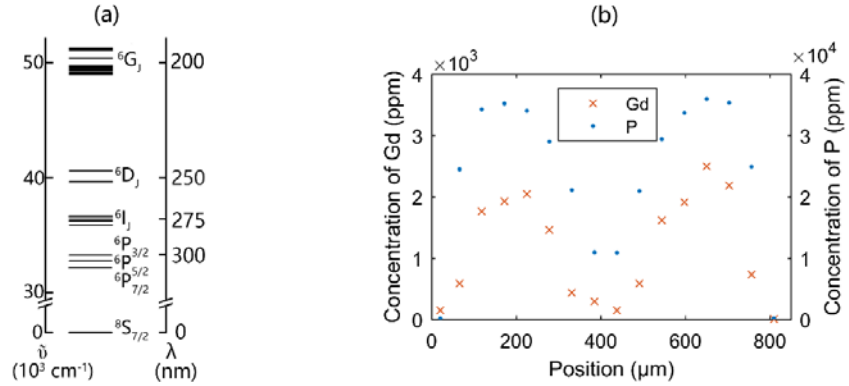

FIG. 1. (a) Gd^{3+} energy levels with wavenumbers ($\tilde{\nu}$) and wavelengths (λ) of the photons emitted in the transition to the ground level (adapted from ref. 19 and 20). (b) EDX scan of the Gd^{3+}-doped phosphosilicate preform core area. The dip at the preform center is commonly observed in MCVD fiber preforms and is attributed to the evaporation of P_2O_5 during consolidation, which also removed Gd^{3+}.

A second fiber was manufactured using the rod-in-tube technique with a fluorosilicate cladding and a silica rod doped with 1000 ppm molar Gd fabricated via sol-gel[21]. Tetramethoxysilane (TMOS) and Gd^{3+} nitrate were put under sol-gel reaction in methanol:water 4:1 solution. After gelation at T~45 ºC, the alcogel was subsequently slowly dried to a xerogel in a thermostatic chamber at the same temperature, and finally densified under controlled atmosphere in a suitable oven at T~1250 ºC and a further final densification was achieved during fiber drawing process at temperature above T~2000 ºC. The Gd-doped sample was pulled into a 500 µm diameter cane.

The transmission spectrum of a 15cm-long phosphosilicate fiber sample (Fig. 2(a)) shows dips at λ~244.8 nm, 247.1 nm, 253.2 nm, 273.4-274.6 nm, 276.4 nm, 279.4 nm, 301.4 nm, 306.3 nm and 311.9 nm, which were attributed to the Gd^{3+} transitions from the fundamental ($^8S_{7/2}$) to the ^6D_J, ^6I_J, ^6P_J levels and are in agreement with the energy levels reported in the literature[19-20] and summarized in Fig.1 (a). The spectrum was collected using a broadband deuterium lamp source (BDS130, BWTEK), a spectrometer (USB4000, Ocean Optics) equipped with a 25 µm slit and a UV transparent fiber for the reference spectrum and power delivery into the sample. Although the host material of the data reported in the literature is different, it is well known that in rare earth ions the 4f electronic states are screened by the outer $5s^2$ and $5p^6$ electron shells, thus the positions of the absorption and emission spectral lines are weakly affected by the host environment. The propagation losses at 309 nm and 317 nm, measured using the cut back method, were estimated to be ~1.8 dB/m and ~1.3 dB/m, respectively. The weaker output at short wavelengths in Fig. 2(a) was mostly attributed to the absorption associated with defects[22] and the bandgap of phosphosilicate glass[23] which can be further optimized. The broad absorption peak centered at λ~250 nm has been attributed to oxygen deficient centers (ODCs) and impeded the loss characterization of the Gd^{3+} transitions from the ground levels to the ^6D_J and ^6I_J via cut back method.

2D photoluminescence (PL) and photoluminescence excitation (PLE) spectral mapping of the phosphosilicate fiber sample (Fig. 2(b)) were recorded at room temperature with a Horiba Fluorolog-3 spectrofluorometer equipped with a xenon excitation lamp, and corrected for excitation spectrum, detector spectral sensitivity and blaze angle of emission grating. In order to improve the signal to noise ratio (SNR) and obtain a significant signal from the fiber sample, a bundle of approximately 10^3 fibers without polymer coating was assembled to form a parallelepiped with dimensions 1 cm x 1 cm x 1 mm (Fig. 3(a)). Light was incident on the fiber side, which has the highest core to cladding aspect ratio. Both the excitation and emission slits were set to 1 nm bandpass with an estimated beam size of 1 mm x 6.5 mm at the sample surface. In the spectral mapping, intense PL emission at λ_{em}~312 nm, given by the $^6P_{7/2} \rightarrow {}^8S_{7/2}$ transition, was observed under excitation at λ_{ex}=272.7 nm and 275.4 nm, i.e., pumping into the Gd^{3+} ^6I_J multiplet levels. A ~1 nm shift from the absorption spectrum was attributed to the different calibrations of the spectrometer and the spectrofluorometer used.

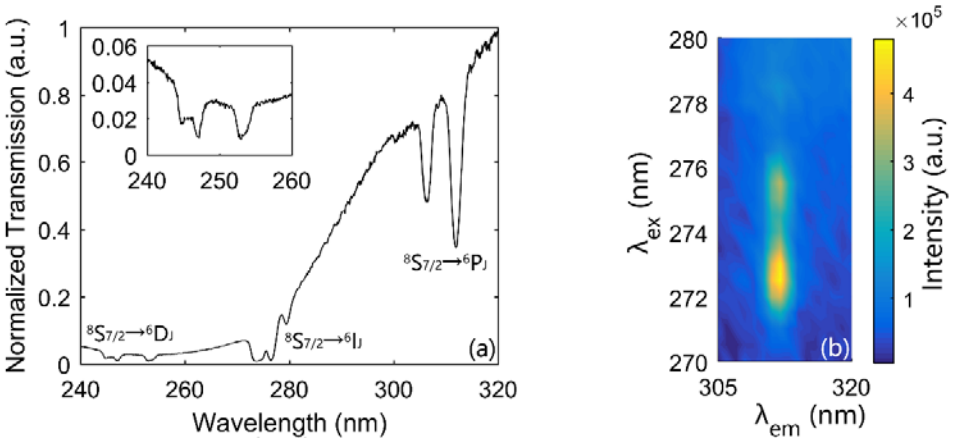

FIG. 2. (a) Phosphosilicate fiber transmission spectrum (b) 2D PL/PLE spectral mapping of the phosphosilicate fiber sample. The excitation and emission mapping step were 0.5 nm and 1nm respectively.

As the fiber drawing process corresponds to a thermal treatment at high temperature, fiber preforms were also analyzed for comparisons. A disk was cut from the phosphosilicate preform with a core diameter of 0.8 mm and its cross-section polished to minimize scattering (Fig. 3(b)). Disks cut from sol-gel silica samples without any cladding layer have been studied in ref. 24.

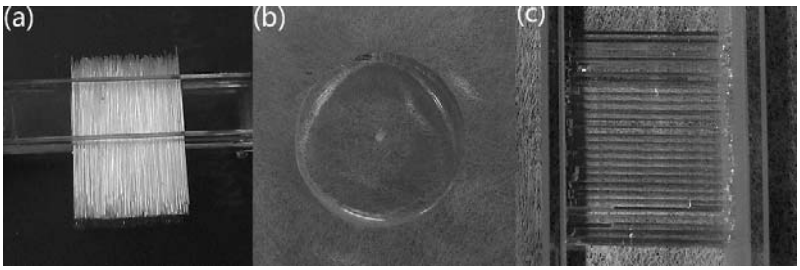

FIG. 3. (a) Phosphosilicate fiber bundle, (b) Phosphosilicate preform disk, and (c) silica fiber bundle hold in a cuvette.

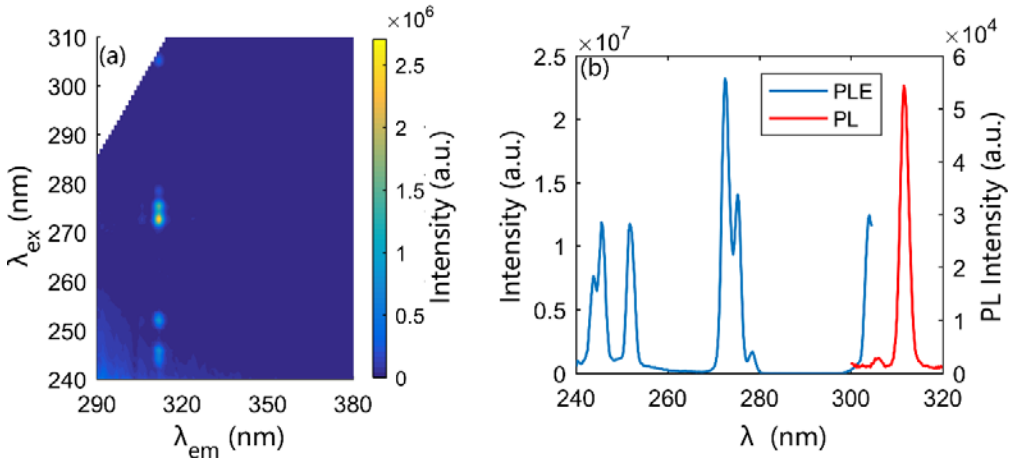

FIG. 4. (a) 2D PL/PLE spectral mapping of the phosphosilicate preform disk. Due to the weak excitation intensity at short wavelengths, mappings were taken on multiple sub-areas with scanning step ranging from 0.5 nm to 2 nm before combination. (b) PL (excitation wavelength λ_{ex}=272.5 nm) and PLE (emission wavelength λ_{em}=312 nm) spectra. Slit widths as well as the peak values differ because of the increased excitation and emission slit widths used for PL and PLE signal optimizations respectively. The wavelength ranges are limited to the data available for correction, based on the wavelength dependent source power and detector sensitivity.

The phosphosilicate preform disk exhibits intense emissions at λ_{em}=311.7 nm, attributed to the Gd^{3+} $^6P_{7/2}\rightarrow{}^8S_{7/2}$ transition, observed under excitations at λ_{ex}=243.7 nm, 245.7 nm and 251.9 nm, attributed to pumping into the ^6D_J levels; excitations at λ_{ex}=272.6 nm, 275.2 nm and 278.3nm, attributed to pumping into the ^6I_J levels; and excitations at λ_{ex}=304.0 nm, attributed to pumping into the $^6P_{5/2}$ levels, respectively (Fig. 4). A comparison with the results obtained for the fiber sample (Fig. 2(b)) suggests that the emission wavelengths, thus the energy levels of the Gd^{3+} dopant, were unaffected by the fiber pulling process performed at high temperature. The $^6P_{7/2}\rightarrow{}^8S_{7/2}$ transition, which features a spin change, is associated with an emission band having a linewidth of $\Delta\lambda$~2.5 nm (FWHM). The relatively strong emission signal at excitation of λ_{ex}=272.5 nm is partly attributed to the dense distribution of energy levels in the ^6I_J energy level group (Fig.1(a)) which results in multiple lines broadened by glass host and overlapping within the bandpass 1 nm wavelength range. At this excitation, a weak emission from the $^6P_{5/2}$ energy level was also observed at λ_{em}~306 nm in the PL spectrum. Excitation to this level, followed by an inter-band non-radiative decay to $^6P_{7/2}$, corresponds to a peak at λ_{em}~304 nm in the PLE spectrum, suggesting a Stokes shift of $\Delta\lambda$~2 nm.

The polished disk sample (Fig. 4(a)) showed a higher SNR than the fiber bundle (Fig. 2(b)). Although the SNR is relatively low at short excitation wavelengths mostly due to the weak intensity of the light source below λ_{ex}~250 nm, a weak signal from ODC(II)[25] was clearly observed as a wide-band emission (see the left bottom of the Fig. 4(a)). Despite of the wide transparency range of pure silica, various types of defects can induce loss in the UV wavelength region. ODC is one of the most common silica defects optically active in the UV region and has attracted

particular interest due to its photoluminescence features[25]. The excitation spectra for two characteristic emission wavelengths of the ODC(II), namely λ_{em}~282 nm and λ_{em}~459 nm[26], was verified (Fig. 5). Its absorption band overlaps with some of the transitions in Gd^{3+}, thus it would affect the pump efficiency in potential applications.

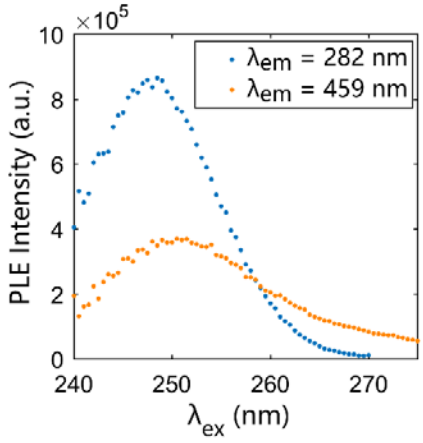

FIG. 5. PLE spectra of ODCs at two emission wavelengths (λ_{em}) in the phosphosilicate preform sample.

The PL/PLE mapping and PL(E) spectra from the Gd^{3+}-doped silica fiber sample were recorded with a wavelength step of 0.5 nm and slit widths of 1nm (Fig. 6). A stack of fifty Gd^{3+}-doped silica fiber canes without polymer coating was prepared to form a parallelepiped with dimensions 1 cm x 1 cm x 1 mm. Results showed an approximately $\Delta\lambda$~1.5 nm shift in the Gd^{3+} emission wavelengths with respect to the phosphosilicate sample. A weak luminescence signal at λ_{em}~325 nm, nearly $\Delta\tilde{\nu}$~1100 cm^{-1} from λ_{em}~314 nm, matches the Raman shift associated to the Si-O-Si fundamental vibration. Compared with the phosphosilicate sample, instead of the ODC(II) emission band, a wide-band emission at λ_{em}~390 nm previously observed in the disk sample[24] was detected here but with its peak intensity reduced to about 1/18 of the peak PL intensity from Gd^{3+}. This wavelength is close to the $T_1 \rightarrow S_0$ transition of the Ge-ODC[27] which was previously detected in silica containing germanium (Ge) impurities at concentrations of the order of 10 ppm by weight[28]. In this preform, Ge might have been induced during preform fabrication using the sol-gel method in the form of impurity in the silicon precursors. However, here the excitation-wavelength-dependent peak position implies a more complex explanation. Since this signal was not observed in the phosphosilicate samples, it is currently supposed to emerge from intrinsic defects of the host. The difference in intensity between Gd^{3+} luminescence and this signal increased in comparison to that recorded in the sol-gel disk sample before fiber drawing process[24]. As the fiber pulling process corresponds to a rapid thermal treatment of the sample, this phenomenon is in accordance with the enhanced Gd luminescence observed in the literature after rapid thermal treatment[17]. Besides, the excitation peak at λ_{ex}=307.5 nm (to $^6P_{5/2}$ level) features a shoulder at 305.5 nm, which is different from the peak profile observed previously. This difference is similar to the host-dependent Er^{3+} $^4I_{13/2} \rightarrow {}^4I_{15/2}$ transition[8]. Both phenomena confirmed that the

Gd^{3+} experience a different surrounding in the silica and phosphosilicate samples[29]. Further analysis on the emission at λ_{em}~390 nm will be carried out in the future.

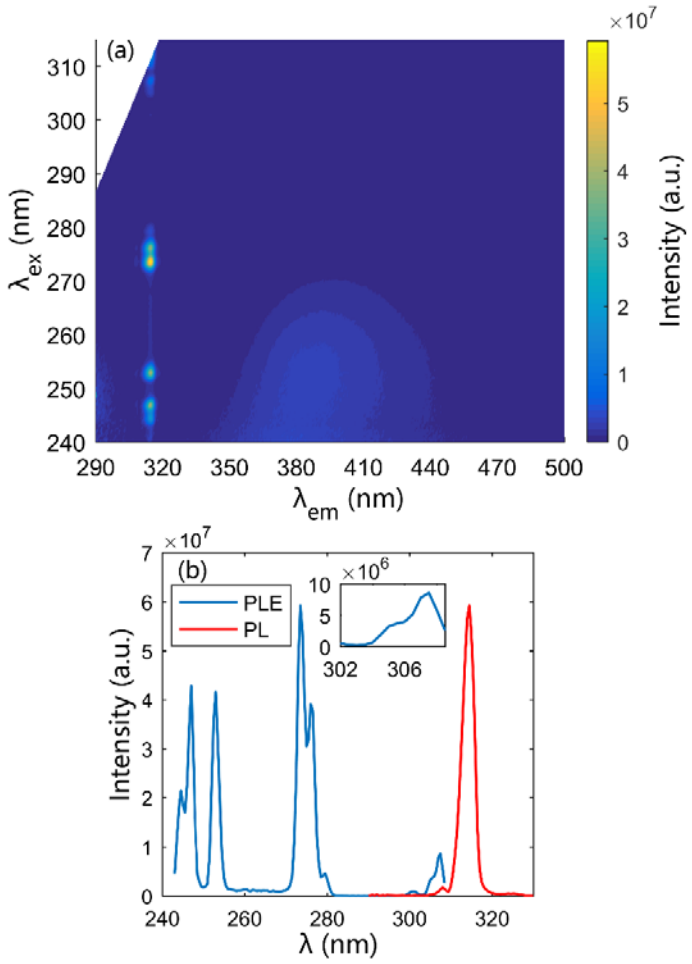

FIG. 6. (a) 2D PL/PLE spectral mapping, (b) PL (λ_{ex}=274 nm) and PLE (λ_{em}=314 nm) spectra of the Gd^{3+}-doped silica fiber sample extracted from 2D mapping.

In conclusion, PL and PLE spectra before and after fiber drawing show that phosphosilicate and pure silica fibers doped with Gd^{3+} are optically active in the UV with emissions observed at λ_{em}~312 and 314 nm when the samples are pumped at λ_{ex}~272.5 nm or 252 nm in the phosphosilicate sample and λ_{em}~274 nm or 253 nm in the silica sample, respectively.

The authors gratefully acknowledge support from Engineering and Physical Sciences Research Council (No. EP/L01243X/1). All data supporting this study are openly available from the University of Southampton repository at http://doi.org/10.5258/SOTON/402084.

[1]K. Song, M. Mohseni, and F. Taghipour, Water Res. **94**, 341 (2016).

[2]T. Bintsis, E. Litopoulou-Tzanetaki, and R.K. Robinson, J. Sci. Food Agric. **80**, 637 (2000).

[3]A. Endruweit, M.S. Johnson, and A.C. Long, Polym. Compos. **27**, 119 (2006).

[4]M. Han, W. Lee, S.-K. Lee, and S.S. Lee, Sensors Actuators, A Phys. **111**, 14 (2004).

[5]J.M. Hoffman, A.K. Hays, and G.C. Tisone, Appl. Phys. Lett. **28**, 538 (1976).

[6]H.M. Pask, P. Dekker, R.P. Mildren, D.J. Spence, and J.A. Piper, Prog. Quantum Electron. **32**, 121 (2008).

[7]G.K. Samanta, S.C. Kumar, A. Aadhi, and M. Ebrahim-Zadeh, Opt. Express **22**, 11476 (2014).

[8]W. Miniscalco, in Rare-Earth-Doped Fiber Lasers Amplifiers, Revis. Expand., edited by M.J.F. Digonnet, Second Edi (CRC Press, New York, 2001).

[9]E. Williams, E.B. Brousseau, and A. Rees, Int. J. Adv. Manuf. Technol. **74**, 769 (2014).

[10]J. Gabzdyl, Nature Photonics **2**, 21 (2008).

[11]G. Siegel, J. Non. Cryst. Solids **13**, 372 (1974).

[12]See https://www.fiberguide.com/wp-content/uploads/2012/09/Solarguide_090712.pdf for attenuation spectrum of commercialized UV fiber from Fiberguide Company (Stirling, New Jersey); accessed 11 Oct 2016

[13]U. Vetter, J. Zenneck, and H. Hofsäss, Appl. Phys. Lett. **83**, 2145 (2003).

[14]Z. Yang, J. Lin, M. Su, Y. Tao, and W. Wang, J. Alloys Compd. **308**, 94 (2000).

[15]Z. Tian, H. Liang, B. Han, Q. Su, Y. Tao, G. Zhang, and Y. Fu, J. Phys. Chem. C **112**, 12524 (2008).

[16]N. Chiodini, M. Fasoli, M. Martini, F. Morazzoni, E. Rosetta, R. Scotti, G. Spinolo, A. Vedda, M. Nikl, N. Solovieva, A. Baraldi, R. Capelletti, and R. Francini, Radiat. Eff. Defects Solids **158**, 463 (2003).

[17]D.Di. Martino, N. Chiodini, M. Fasoli, F. Moretti, A. Vedda, A. Baraldi, E. Buffagni, R. Capelletti, M. Mazzera, M. Nikl, G. Angella, and C.B. Azzoni, J. Non. Cryst. Solids **354**, 3817 (2008).

[18]J.E. Townsend, S.B. Poole, and D.N. Payne, Electron. Lett. **23**, 329 (1987).

[19]G.H. Dieke and H.M. Crosswhite, Appl. Opt. **2**, 675 (1963).

[20]R.T. Wegh, A. Meijerink, R.-J. Lamminmäki, and J. Hölsä, J. Lumin. **87-89**, 1002 (2000).

[21]F. Moretti, N. Chiodini, M. Fasoli, L. Griguta, and A. Vedda, J. Lumin. **126**, 759 (2007).

[22]H. Imai, K. Arai, H. Imagawa, H. Hosono, and Y. Abe, Phys. Rev. B **38**, 12772 (1988).

[23]M. Engholm and L. Norin, Opt. Express **16**, 1260 (2008).

[24]J. He, Y. Wang, S. Steigenberger, A. Macpherson, N. Chiodini, and G. Brambilla, in *Conf. Lasers Electro-Optics* (OSA, Washington, D.C., 2016), p. JTh2A.86.

[25]R. Salh, Cryst. Silicon Prop. Uses 135 (2011). 1 R. Salh, in *Cryst. Silicon - Prop. Uses*, edited by S. Basu (InTech, 2011), pp. 135–172.

[26]L. Skuja, J. Non. Cryst. Solids **239**, 16 (1998).

[27]G. Pacchioni, L. Skuja, and D.L. Griscom, *Defects in SiO_2 and Related Dielectrics: Science and Technology* (Springer Netherlands, Dordrecht, Netherlands, 2000) p.314.

[28]M. Cannas. arXiv preprint cond-mat/0203284 (2002)

[29]A. Saitoh, S. Matsuishi, C. Se-Weon, J. Nishii, M. Oto, M. Hirano, and H. Hosono, J. Phys. Chem. B **110**, 7617 (2006).